

Stereochemical Equivalence of P^{III}-Bonded Hydrogen Atoms and |Se^{IV} Lone Electron Pairs in Sr(H₂PO₃)₂ and Sr(HSeO₃)₂

Kai Boldt,^[a] Bernward Engelen,^{*[a]} Martin Panthöfer,^[a] and Klaus Unterderweide^[a]

Keywords: Hydrogen bonds / IR spectroscopy / Stereochemical equivalence / Strontium / Phosphates / Selenates

Sr(H₂PO₃)₂ and Sr(HSeO₃)₂ have been characterized by means of single crystal X-ray diffraction and FT-IR absorption spectroscopy. The IR spectra exhibit split AB band systems in the OH stretching mode region due to Fermi resonance interactions of the ν(OH) with the in-plane bending modes of the hydroxyl groups. The compounds crystallize in a new structure type and are isotypic, if the P-bonded hydrogen atoms of Sr(H₂PO₃)₂ and the lone electron pairs of Sr(HSeO₃)₂ are considered to be equivalent. The coordination of Sr is that of a distorted square antiprism. The SrO₈ polyhedra share three common edges and are additionally

connected via O–X–O bonds of the isolobal XO₂OH[−] ions (X = HP^{III}, |Se^{IV}) of tetrahedral and trigonal (ψ-tetrahedral) configuration, respectively. The resulting layers $\frac{2}{3}$ [Sr(XO₂OH)₂] are connected via circular hydrogen bond systems of tetrameric [XO₂OH]₄ groups of a cyclooctane like chair topology. Both the P-bonded hydrogen atoms and the lone electron pairs of the HP^{III}O₂OH[−] and the |Se^{IV}O₂OH[−] ions, respectively, form channels along [001] and induce the same crystal structure. This is new for acid salts of the type M^{II}(XO₂OH)₂·nH₂O with X = HP^{III} and |Se^{IV}.

Introduction

Strontium hydrogen phosphate(III), Sr(H₂PO₃)₂, and strontium hydrogen selenate(IV), Sr(HSeO₃)₂, have been isolated by Ebert et al.^[1–4] as part of their studies of the solubility diagrams of the quasiternary systems SrO–P₂O₃–H₂O and SrO–SeO₂–H₂O, respectively. The selenium compound has been characterized by means of thermal analysis as well as IR absorption spectroscopy and some X-ray data.^[4–6] Since the corresponding phosphates(III) tend to form supersaturated solutions, they are difficult to obtain, especially in the form of single crystals. The knowledge about this class of compounds is thus poor.^[1–3] Such acid salts are of special interest because of: i) the strong and medium-strong hydrogen bonds, and hence the formation and transformation of AB and ABC band systems in the OH stretching mode region of the existing hydroxyl groups,^[6,7] ii) the possible stereochemical equivalence of the P-bonded hydrogen atom of the phosphate(III) and the lone electron pair of the selenate(IV), which one can find for some corresponding neutral salts, e.g., for CuHPO₃·2H₂O^[8]/CuSeO₃·2H₂O^[9] and MgHPO₃·6H₂O^[10]/MgSeO₃·6H₂O^[11–12], but not for acid compounds of the type M^{II}(HXO₃)₂·nH₂O (X = HP^{III} and |Se^{IV}), and iii) their possible nonlinear optical and dielectrical properties. In this context we report on the crystal structures and FT-IR absorption spectra of Sr(H₂PO₃)₂ and Sr(HSeO₃)₂.

Results and Discussion

Crystal Structures

Sr(H₂PO₃)₂ (*a*P26) and Sr(HSeO₃)₂ (*a*P22) both crystallize in a triclinic unit cell in the space group *P* $\bar{1}$ with *Z* = 2 (see Table 1). Except for the P-bonded hydrogen atoms of Sr(H₂PO₃)₂ they are isotypic. All atoms occupy general positions 2*i* with Sr²⁺ and two crystallographically different XO₂OH[−] ions with X = HP^{III} and |Se^{IV}, P1, P2, Se1 and Se2, in the asymmetric unit.

In both structures, Sr is square antiprismatically surrounded by eight oxygen atoms of seven different XO₂OH[−] ions (see Figure 1). The isolobal XO₂OH[−] ions have tetrahedral (HPO₂OH[−]) and trigonal pyramidal (ψ-tetrahedral, SeO₂OH[−]) configuration and act as both bidentate and bridging ligands (Figure 1). Due to the mono- and bidentate coordination of Sr through XO₂OH[−] (see Figure 1) the SrO₈ square antiprisms are strongly distorted. The Sr–O distances range from 251 to 276 pm and 254 to 285 pm for the acid phosphate(III) and selenate(IV) compound, respectively (see Table 2). Nevertheless, the respective mean values, 263(10) and 262(10) pm, are nearly equal. They are in the range of the Sr–O distances of other oxosalts of eight-coordinate Sr.^[13–15]

Due to the different coordinations through Sr and H (see Figure 1) the non-hydrogen atoms of the two XO₂OH[−] ions of the asymmetric unit are differently, but only slightly, distorted from the possible *m* symmetry (see Table 2). The mean X–O and X–OH distances (150 and 159 pm for X = HP^{III} and 166 and 178 pm for |Se^{IV}) and O–X–O angles (111 and 101° for X = HP^{III} and |Se^{IV}, respectively) are in good agreement with those found for other acid phosphates(III)^[16] and selenates(IV).^[7,17–19] Although O23 is not coordinated to Sr, the corresponding X–O distance is

^[a] Anorganische Chemie II, Universität Siegen, D-57068 Siegen, Germany
Fax: (internat.) +49-271/740-2555
E-mail: engelen@chemie.uni-siegen.de

Table 1. Data collection and refinement parameters of $\text{Sr}(\text{H}_2\text{PO}_3)_2$ and $\text{Sr}(\text{HSeO}_3)_2$ ^[a]

	$\text{Sr}(\text{H}_2\text{PO}_3)_2$	$\text{Sr}(\text{HSeO}_3)_2$
Formula weight / $\text{g}\cdot\text{mol}^{-1}$	249.59	343.56
Temperature /K	293(2)	293(2)
Wavelength /pm	71.073	71.069
Crystal system, space group	triclinic, $P\bar{1}$	triclinic, $P\bar{1}$
Lattice constants /pm, $^\circ$	$a = 581.3(1)$, $\alpha = 97.69(3)$ $b = 722.5(1)$, $\beta = 104.51(3)$ $c = 806.0(2)$ pm, $\gamma = 106.47(3)$	$a = 586.8(1)$, $\alpha = 97.23(1)$ $b = 727.7(1)$, $\beta = 104.06(1)$ $c = 779.1(1)$, $\gamma = 106.20(1)$
Volume / nm^3	0.3065(1)	0.30314(8)
Z , $\rho_{\text{calc.}}$ / $\text{Mg}\cdot\text{m}^3$	2, 2.704	2, 3.764
Absorption coefficient / mm^{-1}	9.277	20.859
$F(000)$	240	312
Crystal size / mm^3	$0.20 \times 0.19 \times 0.15$	$0.14 \times 0.10 \times 0.10$
Θ_{min} , Θ_{max} / $^\circ$	3.56, 28.05	2.76, 39.97
Index ranges	$-7 \leq h \leq 7$ $-9 \leq k \leq 9$ $-10 \leq l \leq 10$	$-10 \leq h \leq 9$ $-12 \leq k \leq 13$ $-1 \leq l \leq 14$
total reflections	3468	3736
unique reflections, R_{int}	1393, 0.034	2994, 0.052
Completeness to $\Theta = 28.05^\circ$	92.8%	79.9%
Absorption correction	Numerical	Empirical
T_{min} , T_{max}	0.23, 0.31	0.24, 0.28
Refinement method	Full-matrix least-squares on F^2	
Data/restraints/parameters	1393/2/95	2994/2/89
S	1.035	1.072
$R1$, $wR2$ [$I > 2\sigma(I)$]	0.026, 0.055	0.026, 0.048
$R1$, $wR2$ (all)	0.036, 0.058	0.047, 0.052
Extinction coefficient	0.023(3)	0.0127(8)
δ_{min} , δ_{max} / $10^{-6} \text{ e}\cdot\text{pm}^3$	$-0.6(2)$, $0.7(2)$	$-0.9(2)$, $0.8(2)$

[a] Further details of the crystal structure investigations, the atomic coordinates and the displacement parameters can be obtained from the Fachinformationszentrum Karlsruhe, D-76344 Eggenstein-Leopoldshafen (Germany) [Fax: (internat.) +49-7247/808-666; E-mail: crysdata@fiz.karlsruhe.de] on quoting the depository numbers CSD-410936 [$\text{Sr}(\text{H}_2\text{PO}_3)_2$] and CSD-410935 [$\text{Sr}(\text{HSeO}_3)_2$].

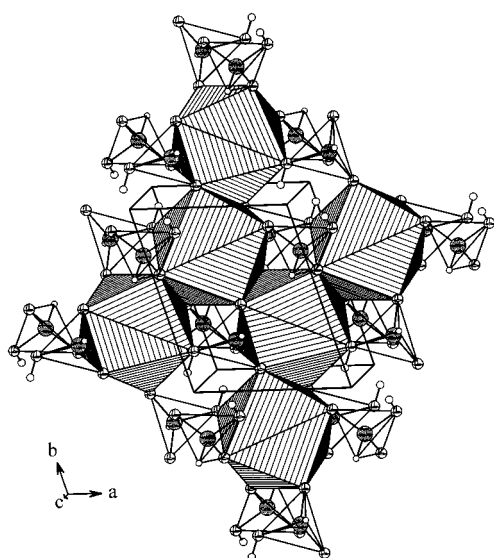


Figure 1. Crystal structure of $\text{Sr}(\text{H}_2\text{PO}_3)_2$ approximately (5°) along $[001]$ representing the SrO_8 polyhedra and their linkage; except for hydrogen atoms H1 and H2, the crystal structure of $\text{Sr}(\text{HSeO}_3)_2$ is identical; the displacement ellipsoids are drawn at a level of 50% probability

only slightly shorter than that of the other hydroxyl group (O13, see Table 2). The dihedral angles $\text{H}-\text{P}-\text{O}-\text{H}$ of the HPO_2OH^- ions (-70 and 64°) point to a *syn-clinal* conformation of the PH and OH groups. This means that the orientation of the HP and OH groups of $\text{Sr}(\text{H}_2\text{PO}_3)_2$ corresponds much better to that found in phosphorous acid,

H_3PO_3 , (76° for the mean value^[20]) than to that found in other acid salts (e.g. 46° in LiH_2PO_3 ^[21]).

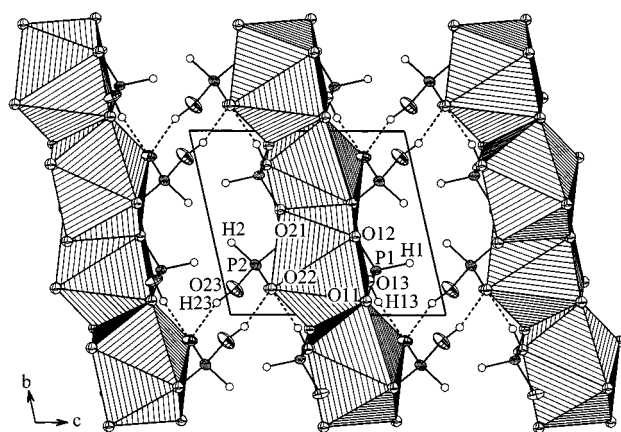
The SrO_8 antiprisms share three edges and are additionally connected via $\text{O}-\text{X}-\text{O}$ bonds with the result that layers ${}_2[\text{Sr}(\text{XO}_2\text{OH})_2]$ are formed parallel to (001) (see Figure 1 and 2). The layers are interconnected via medium-strong hydrogen bonds, $\text{O23}-\text{H23}\cdots\text{O22}$, with $\text{O}-\text{H}\cdots\text{O}$ distances of 277 and 280 pm for $\text{Sr}(\text{H}_2\text{PO}_3)_2$ and $\text{Sr}(\text{HSeO}_3)_2$, respectively, (see Figure 2 and Table 2). Thus the resulting structures are of type $\text{b}1$ ^[22] with respect to the inter-layer forces. A second hydrogen bond, $\text{O13}-\text{H13}\cdots\text{O22}$, appears in the layers with $\text{O}-\text{H}\cdots\text{O}$ distances of 272 and 274 pm, respectively. Thus O22 acts as a hydrogen-bond acceptor for both hydrogen bonds. As a result, a zero-dimensional hydrogen-bond system is formed, in which two XO_2OH^- ions (P2, Se2) form a cyclooctane-like ring system between the layers (see Figure 2 and Figure 3). The XO_2OH^- ions belonging to P1 and Se1, respectively, are connected biaxially to this ring system in the 1,5 position by the intra-layer hydrogen bond (see Figure 2 and 3). Because of the synergetic effect,^[23] i.e., the coordination of O13 through Sr, the intra-layer H-bond ($\text{O13}-\text{H13}\cdots\text{O22}$) is shorter than to the inter-layer H-bond ($\text{O23}-\text{H23}\cdots\text{O22}$) although both hydrogen bonds have the same H-bond acceptor (O22, see Table 2 and Figure 2, 3).

The P-bonded H-atoms (H1 and H2) of $\text{Sr}(\text{H}_2\text{PO}_3)_2$ are not hydrogen-bonded. They are arranged around the centers of symmetry at the 1e (P1) and 1c (P2) positions of the space group $P\bar{1}$, respectively, to form channels along $[100]$

Table 2. Selected interatomic distances (pm) and angles ($^\circ$) for $\text{Sr}(\text{H}_2\text{PO}_3)_2$ and $\text{Sr}(\text{HSeO}_3)_2$

$\text{Sr}(\text{H}_2\text{PO}_3)_2$		$\text{Sr}(\text{HSeO}_3)_2$	
Sr–O₈ square antiprism			
Sr–O11	273.0(3)	Sr–O11	263.4(2)
Sr–O11 ^[a]	252.1(2)	Sr–O11 ^[a]	253.6(2)
Sr–O12	269.9(3)	Sr–O12	282.7(2)
Sr–O12 ^[b]	251.2(2)	Sr–O12 ^[b]	253.6(2)
Sr–O13 ^[c]	275.5(3)	Sr–O13 ^[c]	269.7(2)
Sr–O21 ^[b]	261.8(3)	Sr–O21 ^[b]	258.1(2)
Sr–O21 ^[c]	254.1(3)	Sr–O21 ^[c]	253.7(2)
Sr–O22	268.5(3)	Sr–O22	262.6(2)
XO₂OH[−]			
P1–O11	150.3(2)	Se1–O11	165.6(2)
P1–O12	149.7(2)	Se1–O12	165.7(2)
P1–O13	159.4(3)	Se1–O13	178.9(2)
P1–H1	124(4)		
O11–P1–O12	112.6(2)	O11–Se1–O12	101.0(1)
O11–P1–O13	112.1(1)	O11–Se1–O13	102.4(1)
O12–P1–O13	108.2(1)	O12–Se1–O13	99.7(1)
P2–O21	149.1(3)	Se2–O21	164.8(2)
P2–O22	152.3(2)	Se2–O22	167.4(2)
P2–O23	157.6(3)	Se2–O23	177.6(2)
P2–H2	128(4)		
O21–P2–O22	116.3(2)	O21–Se2–O22	106.3(1)
O21–P2–O23	106.3(2)	O21–Se2–O23	94.78(9)
O22–P2–O23	109.9(1)	O22–Se2–O23	99.9(1)
H-bonds			
O13–H11	88(2)	O13–H1	88.(2)
O13...O22 ^[d]	271.7(3)	O13...O22 ^[b]	274.3(3)
O13–H11...O22 ^[d]	171(5)	O13–H1–O22	163(4)
O23–H21	91(2)	O23–H2	89(2)
O23...O22 ^[e]	276.5(4)	O23...O22 ^[d]	280.3(3)
O23–H21...O22 ^[e]	164(4)	O23–H2...O22 ^[d]	167(4)

^[a] Symmetry operator: $-x+1, -y, -z+1$. – ^[b] Symmetry operator: $-x+1, -y+1, -z+1$. – ^[c] Symmetry operator: $x+1, y, z$. – ^[d] Symmetry operator: $-x, -y, -z+1$. – ^[e] Symmetry operator: $-x, -y, -z$.

Figure 2. Crystal structure of $\text{Sr}(\text{H}_2\text{PO}_3)_2$ along [100] representing the $\text{Sr}(\text{HPO}_2\text{OH})_2$ layers and the hydrogen bonds (dotted lines); see also Figure 1

(see Figure 2). In $\text{Sr}(\text{HSeO}_3)_2$, the free electron pairs of $[\text{Se}^{\text{IV}}]$ are oriented in the same directions as the P–H bonds of $\text{Sr}(\text{H}_2\text{PO}_3)_2$. Because of the P...H and H...H repulsion of the nonbonded P and H atoms around the channels along [100], the mean values of the accompanying smallest P...P and Se...Se distances, are 12% larger in $\text{Sr}(\text{H}_2\text{PO}_3)_2$ (479 pm) than in $\text{Sr}(\text{HSeO}_3)_2$ (427 pm). This gives an explanation for the finding that, despite the much longer Se–O distances, the cell volume is smaller in the selenate(IV) compound (see

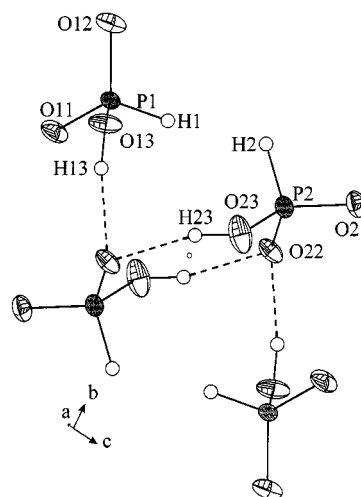
Figure 3. Zero-dimensional hydrogen bond system of $\text{Sr}(\text{H}_2\text{PO}_3)_2$; see also Figure 1

Table 1 and 2). Nevertheless, the interlayer hydrogen bond ($\text{O23}–\text{H23} \cdots \text{O22}$) is shorter for $\text{Sr}(\text{H}_2\text{PO}_3)_2$, i.e., the oxygen atoms of HPO_2OH^- are stronger H-bond acceptors than those of SeO_2OH^- (see also^[23,24]).

Vibrational Spectroscopy

The IR absorption spectra of $\text{Sr}(\text{H}_2\text{PO}_3)_2$ and $\text{Sr}(\text{HSeO}_3)_2$ at low (100 K) and room temperature are shown in Figure 4. The band assignment is given in Table 3. The IR spectra of acid salts are well-known for the splitting of the OH stretching modes, $\nu(\text{OH})$, of hydroxyl groups into AB or ABC band systems (see ref.^[6] and the literature cited therein). The broad bands around 3000 and 2350 cm^{-1} in the spectra of $\text{Sr}(\text{HSeO}_3)_2$ can be assigned to such an AB band system. Due to the two different hydroxyl groups of the asymmetric unit, both the A and B bands are split into at least two bands. The IR spectra of $\text{Sr}(\text{H}_2\text{PO}_3)_2$ also exhibit broad absorptions around 3000 cm^{-1} belonging to an A band, but the B band region is dominated by the PH stretching modes of the phosphate(III) groups.

In the region of the in-plane bending mode bands, $\delta(\text{OH})$, of the hydroxyl groups for both compounds, band doublets appear between 1150 and 1250 cm^{-1} . Like the splitting of the PH stretching modes (see Figure 4 and Table 3), the appearance of these doublets confirms the presence of two crystallographically different hydroxyl groups and XO_2OH^- ions. The frequencies of the B bands of $\text{Sr}(\text{HSeO}_3)_2$ are slightly lower than the first overtones of the $\delta(\text{OH})$ frequencies, pointing to a Fermi resonance interaction of the in-plane bending modes with the $\nu(\text{OH})$ of the hydroxyl groups (see also ref.^[6]).

Between 680 and 750 cm^{-1} a similar doublet is observed in the IR spectra of $\text{Sr}(\text{H}_2\text{PO}_3)_2$, which has to be assigned to the out-of-plane bending modes, $\gamma(\text{OH})$, of the hydroxyl groups. The band at 689 cm^{-1} in the LT spectrum of $\text{Sr}(\text{HSeO}_3)_2$ can also be assigned to one of the $\gamma(\text{OH})$ modes. The corresponding high frequency $\gamma(\text{OH})$ band is covered by the SeO stretching modes of the SeO_2OH^- ions.

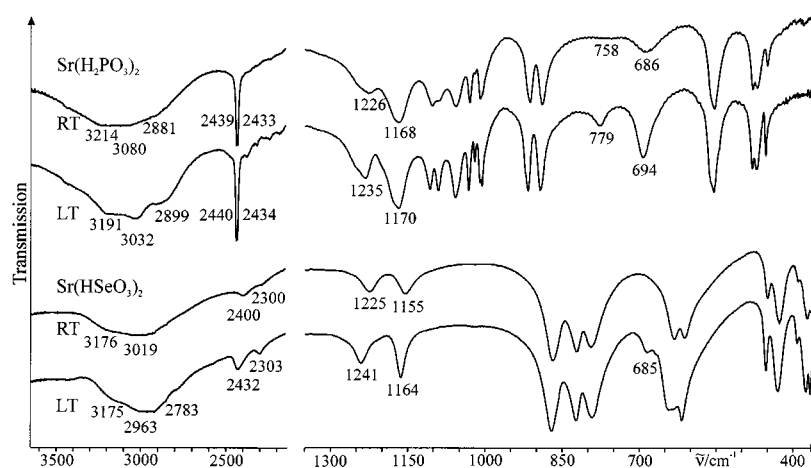


Figure 4. FT-IR absorption spectra at 100 K (LT) and room temperature (RT) of $\text{Sr}(\text{H}_2\text{PO}_3)_2$ and $\text{Sr}(\text{HSeO}_3)_2$

Table 3. Position and assignment of the IR absorption bands of $\text{Sr}(\text{H}_2\text{PO}_3)_2$ and $\text{Sr}(\text{HSeO}_3)_2$

$\text{Sr}(\text{H}_2\text{PO}_3)_2$		$\text{Sr}(\text{HSeO}_3)_2$		Assignment
LT	RT	LT	RT	
3191	3214	3175	3176	$\nu(\text{OH})_{\text{A}}$
3032	3080	2963	3019	
2899	2881	2783		
2440	2439			$\nu(\text{PH})$
2434	2433			
		2432	2400	$\nu(\text{OH})_{\text{B}}/2\delta(\text{OH})$
		2303	2300	
1235	1226	1241	1225	$\delta(\text{OH})$
1170	1168	1164	1155	
1107	1103			$\nu(\text{PO}) + \delta(\text{HPO})$
1091	1090			
1058	1058			
1033	1031			
1021	1020			
1008	1010			
917	914			
894	890			
		871	869	
		823	822	
		792	794	$\gamma(\text{OH})$
779	758			
694	686	685		$\nu(\text{SeO})_{\text{SeOH}}$
		643	632	
		618	612	
556	554			$\delta(\text{OPO})$
480	479			
472	471			$\delta(\text{OSeO})$
		454	450	
		430	427	
		392	390	
		375	372	
		367	360	

Taking into account that both the $\delta(\text{OH})$ and the $\gamma(\text{OH})$ are shifted to higher frequencies, if the respective hydrogen bond is strengthened and shortened, (see refs.^[6,25]), the high frequency $\delta(\text{OH})$ and $\gamma(\text{OH})$ bands can be assigned to the stronger intra-layer hydrogen bond $\text{O13}-\text{H13}\cdots\text{O22}$, whereas the respective low frequency bands belong to the weaker inter-layer hydrogen bond $\text{O23}-\text{H23}\cdots\text{O22}$. For both compounds, the respective pairs $\delta(\text{OH})/\text{d}(\text{O}\cdots\text{O})$ and $\gamma(\text{OH})/\text{d}(\text{O}\cdots\text{O})$ fulfil the corresponding frequency vs.

$\text{O}-\text{H}\cdots\text{O}$ distance correlations (see refs.^[6,25] and the literature cited therein).

Experimental Section

Single crystals of $\text{Sr}(\text{H}_2\text{PO}_3)_2$ and $\text{Sr}(\text{HSeO}_3)_2$ were obtained from concentrated aqueous solutions of $\text{Sr}(\text{H}_2\text{PO}_3)_2$ and $\text{Sr}(\text{HSeO}_3)_2$ at 80 and 22 °C after 3 and 22 days, respectively (see also refs.^[1,6]).

X-ray powder diffraction data for the lattice parameter refinement have been determined from X-ray powder diffractograms ($\text{Cu}-K\alpha_1$ radiation) using a Siemens D5000 X-ray powder diffractometer. For the profile fitting and the refinement of the lattice parameters the program package WinXPow^[26] was used.

The X-ray intensities for the structure determination of $\text{Sr}(\text{H}_2\text{PO}_3)_2$ were collected on a STOE-IPDS image-plate diffractometer ($\text{Mo}-K\alpha$, graphite monochromator) in the oscillation mode. After data reduction a numerical absorption correction based on an experimental crystal description was applied.^[27] The X-ray intensities for the structure determination of $\text{Sr}(\text{HSeO}_3)_2$ were collected on an Enraf–Nonius CAD4 diffractometer ($\text{Mo}-K\alpha$, graphite monochromator). After data reduction, an empirical absorption correction^[28] was applied.

The structures were solved by direct methods and subsequent Fourier syntheses, and refined by full-matrix least-squares techniques with anisotropic displacement parameters for the non-hydrogen atoms using the programs SHELXS97^[29] and SHELXL97.^[30] All hydrogen atoms were located from difference Fourier maps. The coordinates of the hydrogen atoms bonded to phosphorous were refined with isotropic displacement parameters fixed at 1.2 times the equivalent isotropic displacement parameter of the bonded phosphorous atom. All hydrogen atoms bonded to oxygen were refined to an $\text{O}-\text{H}$ distance of 92 pm (DFIX restraint) and isotropic displacement parameters were fixed at 1.5 times the equivalent isotropic displacement parameter of the bonded oxygen atom. Scattering factors for neutral atoms were used.^[31] An empirical extinction correction had to be applied.^[30] Graphics were obtained with DIAMOND 2.1.^[32] Further details of data collection and refinement are given in Table 1.

FT-IR absorption spectra were recorded on a Bruker IFS 113v Fourier-Transform spectrometer equipped with a Graseby-Specac P/N 21.500 cryostat using the KBr-disc method.

Acknowledgments

The authors wish to thank the Deutsche Forschungsgemeinschaft and the Fonds der Chemischen Industrie for financial support.

- [1] Z. Dlouhý, M. Ebert, V. Veselý, *Coll. Czech. Chem. Commun.* **1959**, 24, 2801–2802.
- [2] M. Ebert, J. Eyseltová, A. Rottová, *Coll. Czech. Chem. Commun.* **1970**, 35, 1824–1831.
- [3] I. Lukes, M. Ebert, *Coll. Czech. Chem. Commun.* **1980**, 45, 2283–2289.
- [4] M. Ebert, D. Havlicek, *Coll. Czech. Chem. Commun.* **1982**, 47, 1923–1930.
- [5] T. Losoi, J. Valkonen, *Finn. Chem. Lett.* **1985**, 1, 1–8.
- [6] K. Unterderweide, B. Engelen, K. Boldt, *J. Mol. Struct.* **1994**, 322, 233–239.
- [7] B. Engelen, K. Boldt, H. Müller, K. Unterderweide, *J. Mol. Struct.* **1997**, 436–437, 247–256.
- [8] M. Handlovic, *Acta Crystallogr. B* **1969**, 25, 227–231.
- [9] G. Gattow, *Acta Crystallogr.* **1958**, 11, 377–383.
- [10] D. E. C. Corbridge, *Acta Crystallogr.* **1956**, 9, 991–994.
- [11] R. Weiss, J.-P. Wendling, D. Grandjean, *Acta Crystallogr.* **1966**, 20, 563–566.
- [12] L. Andersen, O. Lindqvist, J. Moret, *Acta Crystallogr. C* **1984**, 40, 586–589.
- [13] A. Boudjada, R. Masse, J. C. Guitel, *Acta Crystallogr. B* **1978**, 34, 2692–2695.
- [14] M. A. Simonov, S. I. Troyanov, E. Kemnitz, D. Hass, M. Kammler, *Kristallografiya* **1988**, 33, 145–146.
- [15] H. Effenberger, *Acta Crystallogr. C* **1987**, 43, 182–184.
- [16] J. Loub, *Acta Crystallogr. B* **1991**, 47, 468–473.
- [17] K. Boldt, B. Engelen, K. Unterderweide, *Acta Crystallogr. C* **1997**, 53, 666–668.
- [18] K. Boldt, B. Engelen, H. Müller, M. Panthöfer, K. Unterderweide, *J. Mol. Struct.* **1999**, 475, 35–41.
- [19] B. Engelen, K. Boldt, K. Unterderweide, U. Bäumer, *Z. Anorg. Allg. Chem.* **1995**, 621, 331–339.
- [20] G. Becker, H. D. Hausen, O. Mundt, W. Schwarz, C. T. Wagner, *Z. Anorg. Allg. Chem.* **1990**, 591, 17–31.
- [21] G. B. Johansson, O. Lindqvist, *Acta Crystallogr. B* **1976**, 32, 412–414.
- [22] A. F. Wells, *Structural Inorganic Chemistry*, 4th ed., Clarendon Press, Oxford, **1975**, pp. 30–33.
- [23] H. D. Lutz, *Struct. Bonding* **1988**, 69, 97–125.
- [24] H. D. Lutz, K. Beckenkamp, H. Möller, *J. Mol. Struct.* **1994**, 322, 263–266.
- [25] H. Ratajczak, W. J. Orville-Thomas, *J. Mol. Struct.* **1967–68**, 1, 449–461.
- [26] STOE & CIE, WinXPow, Darmstadt, **1999**.
- [27] STOE & CIE, XSHAPE 1.02, Darmstadt, **1997**.
- [28] A. C. T. North, D. C. Philips, F. S. Matthews, *Acta Crystallogr. A* **1968**, 24, 351–359.
- [29] G. M. Sheldrick, SHELXS-97, *Program for the solution of Crystal Structures*, University of Göttingen, Germany, **1997**.
- [30] G. M. Sheldrick, SHELXL-97, *Program for Structures Refinement*, University of Göttingen, Germany, **1997**.
- [31] *International Tables for X-ray Crystallography, Vol. C*, (Ed.: A. J. C. Wilson), Kluwer Academic Publishers, Dordrecht, **1995**.
- [32] Crystal Impact, DIAMOND 2.1, Bonn, **1999**.

Received February 17, 2000
[O00057]